Development 118, 1013-1023 (1993)
Printed in Great Britain © The Company of Biologists Limited 1993

Mechanical evaluation of theories of neurulation using computer simulations

David A. Clausi[1] and G. Wayne Brodland[2,*]

[1]Department of Systems Design Engineering, University of Waterloo, Waterloo, Ontario, N2L 3G1, Canada
[2]Departments of Civil Engineering and Biology, University of Waterloo, Waterloo, Ontario, N2L 3G1, Canada

*Author for correspondence

SUMMARY

Current theories about the forces that drive neurulation shape changes are evaluated using computer simulations. Custom, three-dimensional, finite element-based computer software is used. The software draws on current engineering concepts and makes it possible to construct a 'virtual' embryo with any user-specified mechanical properties. To test a specific hypothesis about the forces that drive neurulation, the whole virtual embryo or any selected part of it is ascribed with the force generators specified in the hypothesis. The shape changes that are produced by these forces are then observed and compared with experimental data.

The simulations demonstrate that, when uniform, isotropic circumferential microfilament bundle (CMB) constriction and cephalocaudal (axial) elongation act together on a circular virtual neural plate, it becomes keyhole shaped. When these forces act on a spherical (amphibian) embryo, dorsal surface flattening occurs. Simulations of transverse sections further show that CMB constriction, acting with or without axial elongation, can produce numerous salient transverse features of neurulation. These features include the sequential formation of distinct neural ridges, narrowing and thickening of the neural plate, skewing just medial to the ridges, 'hinge' formation and neural tube closure. No region-specific 'programs' or non-mechanical cell-cell communications are used. The increase in complexity results entirely from mechanical interactions. The transverse simulations show how changes to the driving forces would affect the patterns of shape change produced.

Hypotheses regarding force generation by microtubules, intercellular adhesions and forces extrinsic to the neural plate are also evaluated. The simulations show that these force-generating mechanisms do not, by themselves, produce shape changes that are consistent with normal development. The simulations support the concept of cooperation of forces and suggest that neurulation is robust because redundant force generating mechanisms exist.

Key words: neurulation, theories of neurulation, mechanics, computer simulations, finite element method

INTRODUCTION

Neurulation, one of the earliest of developmental processes, has intrigued observers for millennia. The forces that drive the seemingly simple shape changes that are necessary for successful neural tube closure have been a subject of intensive investigation during approximately the last one hundred years (His, 1874; Roux, 1888; Lewis, 1947; Burt, 1943; Jacobson, 1978; Lee and Nagele, 1988; Koehl, 1990; Schoenwolf and Smith, 1990). The general pattern of neural plate shape change has been established (Jacobson, 1962; Burnside and Jacobson, 1968; Jacobson and Löfberg, 1969). Much is also now known about the morphology (Fig. 1A) and mechanical nature of the cytoskeleton and other force-producing structures that affect the neural plate (Burnside, 1973; Gordon and Brodland, 1987; Gordon and Essner, 1987). That neural tube defects are among the most common of human birth defects has, no doubt, provided much of the motivation for this work (Campbell et al., 1986; Copp et al., 1990).

An understanding of neurulation that is consistent with the plethora of experimental evidence has, however, continued to elude researchers (Trinkaus, 1984). The importance to neural tube morphogenesis of the notochord (Youn and Malacinski, 1981; Jacobson, 1984), other extrinsic forces (Lee and Nagele, 1988; Smith and Schoenwolf, 1991) and even microfilaments (Burnside, 1973; Nagele and Lee, 1980; Schoenwolf et al., 1988) remain disputed. Novel theories have arisen to account for intriguing aspects of neural tube closure, such as cell skewing at the junction between the neural plate and neural ridge (Jacobson et al., 1986), and the appearance of 'hinges' during neural tube closure (Smith and Schoenwolf, 1991).

To investigate the mechanics of neurulation, one might construct a physical machine, like Lewis (1947). Gears, levers, springs, shock absorbers and blocks of viscoelastic

materials might be used to model the behaviour of the passive cytoplasmic components and motors or servo-controlled hydraulic cylinders used to produce any forces exerted by microfilaments and microtubules (Fig. 1B). In addition, a small-scale crawler tractor track system might be used between the model cells to exert any forces produced by intercellular adhesion forces or cortical tractoring. To model the neural plate properly, the machine would have to contain many hundreds of modules arranged in a three-dimensional array so as to correspond geometrically to an early stage neural plate. The machine could be used to test various specific hypotheses about the forces that produce neurulation. For example, when a particular set of force generators is activated and the machine is run, it would undergo a sequence of shape changes that corresponds to the shape changes that an embryo with those properties would undergo under the action of those forces.

A computer simulation is a 'virtual' machine, which can be given all of the properties and features of the mechanical contrivance described above. Many of the drawbacks of the physical machine, such as construction cost, friction and self-weight can be eliminated. More sophisticated control systems can be specified and changes can be implemented more easily. Indeed, one might consider a computer simulation to be a 'virtual' embryo, on which hypothetical or real mechanical, biochemical or electrical properties can be imposed and the consequent behaviour ascertained.

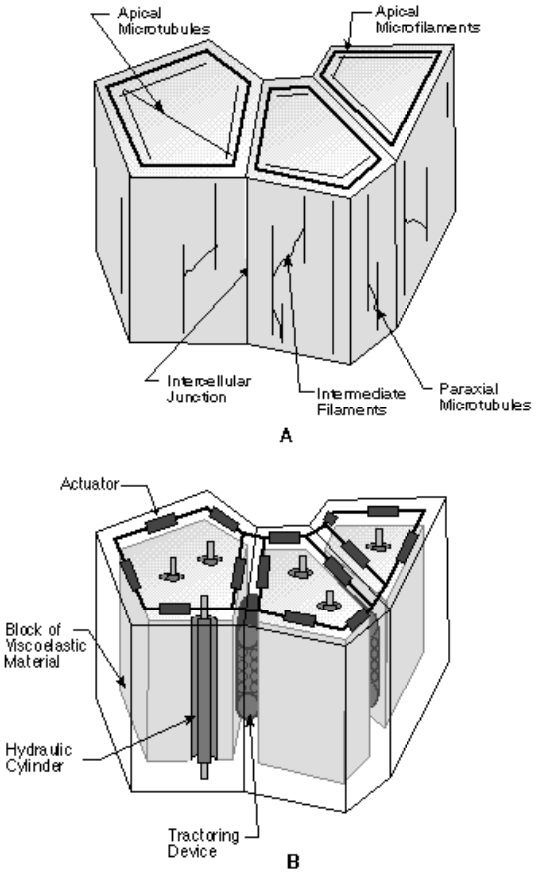

Fig. 1. (A) A schematic of part of an epithelial cell sheet. Cytoskeletal components and some other possible sources of force generation are shown. (B) A corresponding machine. Hydraulic cylinders, for example, act to produce the transverse forces which paraxial microtubules would exert. (These cylinders would act against unbending apical and basal plates which are not shown.) The forces generated by apical microfilaments and microtubules could be generated in the analogous machine by servo-mechanical actuators. A tractoring device serves to drive relative intercellular motions.

Computer simulations play an important role in advancing our understanding of neurulation and other developmental processes (Jacobson and Gordon, 1976; Odell et al., 1981; Hilfer and Hilfer, 1983; Jacobson et al., 1986; Weliky and Oster, 1990; Clausi, 1991; Brodland, 1993; Brodland and Clausi, 1993). In particular, they provide a means to test our intuitive understandings of developmental processes. 'Without such computer simulations, we are only engaging in handwaving and wishful thinking about the performance of our models [hypotheses]' (Gordon, 1985). A formulation that can test the spectrum of current hypotheses about the forces that drive neurulation was required (Jacobson, 1980; Koehl, 1990).

Here, we use a finite element-based computer simulation to investigate a number of hypotheses about the forces that drive neurulation. The kinds of driving forces specified in each of a number of different theories are applied in turn and the patterns of shape change that they produce in a virtual embryo are observed. Different driving forces are found to produce significantly different patterns of shape change. The simulations support aspects of the traditional view and aspects of the modern concepts of cooperation of forces and regional differences (Brun and Garson, 1984; Schoenwolf and Smith, 1990). The simulations also suggest the existence of redundant forces and a mechanical reason that embryogenesis is robust. In addition, the simulations make it possible to predict how normal patterns of shape change would be affected if specific force generators are impaired.

FORMULATION

The finite element method (FEM) is a powerful and well-established methodology for modelling physical systems (Abel et al., 1981; Zienkiewicz and Taylor, 1989, 1991). It has been recognized that computer simulations that use the FEM and related numerical methods have potential to elucidate features of developmental processes (Jacobson, 1980; Gordon, 1985; Cheng, 1987a,b; Koehl, 1990; Brodland, 1993; Brodland and Clausi, 1993).

A number of technical challenges arise when the FEM is used to model the mechanics of developmental processes. These arise because large deflections, large strains and cell-cell neighbour changes occur (Brodland, 1993). In addition, cells and their components can exhibit nonlinear material properties and can be incompressible (Brodland and Clausi, 1993).

A continuum-based finite element formulation specifically designed to meet these technical challenges and to model the mechanical behaviour of assemblages of cells, including cell sheets, was recently developed by Brodland and Clausi (1993). The formulation is truly three-dimensional, satisfies the technical requirements outlined by Gordon (1985) and the authors (Brodland and Clausi, 1993), and allows simulation time steps to be compared directly to the biological time course. Large deflection, large strain and material nonlinearity are accommodated by using an iterative,

updated Lagrangian formulation. Numerical difficulties which can arise when incompressible materials are modelled are circumvented using single-point quadrature and anti-hourglassing procedures (Brodland and Clausi, 1993). The particular formulation used here has been validated by comparison with analytical and numerical solutions (Clausi, 1991) and its efficacy to model developmental processes demonstrated (Brodland and Clausi, 1993). To ensure accuracy, small time steps are used and relevant mechanical features such as constancy of element volumes are checked. Also, a sufficiently fine finite element mesh is used that the results are not mesh dependent.

A neural plate can consist of thousands or tens of thousands of cells, depending on its species and stage of development. To model each cell individually like Weliky and Oster (1990) is impractical due to current computer hardware limitations. The mechanical effect of cell-cell rearrangements and of cytoplasmic deformations is modelled by an effective isotropic viscosity (Phillips and Steinberg, 1978) and an equivalent stress in the direction of the rearrangement (Brodland and Clausi, 1993). The formulation does not explicitly model sliding between cells. However, since the displacement fields are generally smooth and highly similar from embryo to embryo (Burnside and Jacobson, 1968), it is possible to approximate the real behaviour by a bulk or continuum phenomenon.

Here, we model small patches of cells using volume finite elements. Since each region of the neural plate maintains its volume during neurulation (Burnside and Jacobson, 1968; Keeton and Gould, 1986), constant-volume finite elements of effective viscosity, μ, are used. Circumferential microfilament bundles (CMBs) inscribe the apex of neural plate cells (Burnside, 1971; Gordon and Essner, 1987). Apical and paraxial microtubules are also present. Subjacent to the epithelium are mesoderm and endoderm which together are approximately the same thickness as the overlying pseudostratified neural plate (Burnside and Jacobson, 1968; Burnside, 1971).

Microfilaments have a number of characteristic mechanical properties. The stress, σ, in a microfilament bundle apparently remains constant as it deforms (Rappaport, 1977; Gordon and Brodland, 1987). Also, as a microfilament bundle changes length, its cross-sectional area changes so as to maintain its volume (Burnside, 1971). Thus, the force, F_{MF} produced by a particular segment of a microfilament bundle is assumed to be given by

$$F_{MF} = \sigma A = \sigma A_o \frac{L_o}{L}, \tag{1}$$

where A is the current cross-sectional area of the segment of CMB, L_o is its original length, A_o is its original cross-sectional area and L is its current length. Note, that as a microfilament bundle shortens, the force it exerts increases. It is not physically reasonable that this force increases without bound. Thus, when any microfilament shortens to 15 percent of its original length (Burnside, 1971), it is made stiff. In one of the simulations, microfilament bundles are assumed to exert a force that is independent of their length and which is given by

$$F_{MF} = \sigma A_o. \tag{2}$$

Appropriately oriented, two-noded truss elements are used to model the forces exerted by microtubules and microfilament bundles. We note also that, while CMBs cause apical constriction forces, apical microtubules would cause apical expansion forces if they grew longer and pushed against the cell boundaries. It is the difference between these forces that we assume drives cell apical constriction (Gordon and Brodland, 1987).

In order to simulate a wide range of different behaviours using relatively few simulations, we make use of dimensionless parameters F_A and F_T to describe 'apical' and 'transverse' forces. The ratio, F_A, of net apical force to effective viscosity is defined using the formula

$$F_A = \frac{N_{MF} F_{MF} - N_{AMT} F_{MT}}{\mu w h \theta}, \tag{3}$$

where N_{MF} and N_{AMT} are the mechanically equivalent number of microfilament bundles and apical microtubules, respectively, acting in the direction of the force being calculated. The variables h and w are the initial cell sheet thickness and the initial width of the cross-section of the sheet over which N_{MF} microfilaments and N_{AMT} microtubules act. This width may be chosen to correspond to either a single cell or a patch of cells. In the strip simulations shown below, w corresponds to the width of the strip. A time parameter, θ, with units of time^{-1} makes the parameter, F_A, dimensionless. Dimensionless time, τ, is related to real developmental time, t, by

$$t = \frac{\tau}{\theta}. \tag{4}$$

Brodland and Clausi (1993) have noted that the forces produced by paraxial microtubules, intercellular adhesion forces and several other force generators are mechanically equivalent. Here, we define an equivalent transverse force, F_T, given by

$$F_T = \frac{\eta d + N_{PMT} F_{MT}}{\mu w d \theta}, \tag{5}$$

where η is the adhesion force per unit length of element boundary, d is the current length of this boundary and N_{PMT} is the mechanically equivalent number of paraxial microtubules acting in the direction of the force being calculated.

SIMULATIONS

In each of the simulations described here, a particular, hypothesized combination of driving forces is applied to a whole or partial virtual embryo. In order to provide accurate simulations while keeping computer run times reasonable, neural plate shaping and transverse section shape changes are treated separately. All of the simulation results shown are computer-generated drawings of the actual deformed finite element mesh geometries.

When apical constrictions act, they are assumed to be isotropic and to act with an initial force of $F_A = 0.10$ at all points over the dorsal surface. This value is conservative, for if estimates such as $\sigma = 1.3 \times 10^{-3}$ dynes/μm^2 (Gordon and Brodland, 1987), $A_o = 2.26 \times 10^{-2}$ μm^2 (Burnside, 1971) and $\mu = 2.77 \times 10^{-10}$ dyne·hour/μm^2 (Hiramoto, 1969) are used, although they are for different species (the viscosity measurement is from a different phylum), a parameter as high as $F_A = 80$ can result. In most of the simulations, some form of axial elongation also occurs.

Shaping of the neural plate

Shaping of the initially circular neural plate into a keyhole shape is one of the earliest features of neurulation. To investigate this process, we follow the approach of Jacobson and Gordon (1976) and study this process using a flat plate. Fig. 2 shows a simulation of the left half of the flat dorsal surface of an *Ambystoma mexicanum* (axolotl)

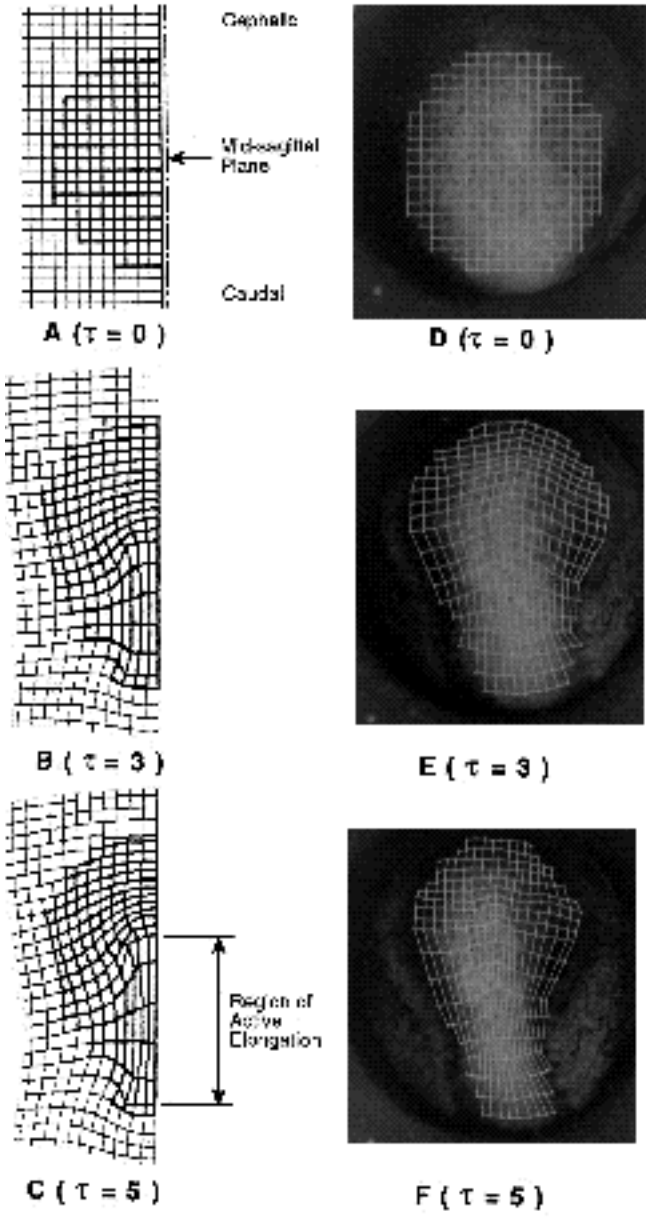

Fig. 2. (A-C) Results of a finite element simulation in which notochord and apical forces act on a flat virtual embryo. The patterns of shape change are evident from the displacements of the finite element boundaries. The parameter τ is a dimensionless time. (D-F) Corresponding time-lapse photographs of axolotl embryo development. Cell motions were tracked manually and used to deform the reference grid shown in D as the embryo developed.

embryo as it develops from approximately stage 14 to stage 16 (Bordzilovskaya et al., 1989). Volume finite elements represent patches of cells, which are initially 80 μm by 80 μm by 120 μm thick. To provide appropriate boundary conditions, the mesh extends to a radius of 1600 μm, the approximate half-circumference of an axolotl embryo. Truss elements (identified with thicker lines in Fig. 2A-C) model the forces produced by CMBs and act only at the apices of the elements which represent patches of neural plate cells. In addition, the region identified in Fig. 2C is elongated at a rate of 100 μm/hour. This region falls inside the physical location of the notochord as identified by Youn et al. (1980) and approximately matches the narrower width of active elongation region identified by Jacobson and Gordon (1976).

Corresponding time-lapse photographs of the dorsal surface of axolotl embryos taken in our laboratory are shown in Fig. 2D-F. A regular grid was placed on the first figure and deformed manually to match subsequent cell motions. Parts A, B and C of the figure correspond in development to parts D, E and F, respectively. Since shape changes occur in the virtual embryo at a rate that matches the time scale of real embryo development, this suggests that the ratio of microfilament force to viscosity that occurs in axolotl neural plate cells is such that F_A 0.10.

Fig. 2 pairs (A,D, B,E and C,F) match, respectively, the in-plane *Taricha torosa* neural plate shape changes reported in parts A,C and D of figure 2 of Burnside and Jacobson (1968). Substantial agreement exists between the three sets of data, both in terms of gross shape changes and details of the shape changes. The patterns of neural plate thickening and thinning produced in the virtual embryo also match the experimental results of Burnside and Jacobson (1968) in that moderate thinning occurs in the dorsal region during shaping and significant thickening occurs in the cephalic region. Furthermore, the regions of thinning and thickening are clearly demarcated at the cephalic end of the actively elongating region in both cases.

The rate of neural plate shaping in *A. mexicanum* is substantially higher than that in *T. torosa* although the patterns of shape change are similar. The parameter, θ, can therefore be used to make the dimensionless time course of the simulation match the real time course of the development of either species. If, for example, θ is set to 0.5 hour^{-1}, real time is (2τ) hour and the simulation approximately matches the development of *T. torosa*, instead.

This simulation makes use of slightly more than 5000 degrees of freedom, requires approximately 20 minutes per time step on a Sun SPARC 1+ computer workstation, for a total run time of approximately five hours.

Do notochord elongation and isotropic microfilament forces acting together also produce out-of-plane shape changes matching those that typically occur in spherical, amphibian embryos? To answer this question, we model a 2 mm diameter, amphibian embryo (Fig. 3). Because of its bilateral symmetry, only one symmetric half of the embryo need be modelled. A 120 μm-thick outer layer, representing the ectodermal layer and a fraction of the underlying mesoderm is given a viscosity, μ. The interior of the real embryo is filled with cells and fluid and is much less resistant to deformation. It is modelled using finite elements that have a viscosity of μ/100. The inner layers of finite elements are required to maintain constancy of embryo volume. An isotropic apical constriction of magnitude F_A=0.10 acts over the presumptive neuroepithelium (the dorsal hemisphere). To avoid confusion with notochord elements, these are not shown with thicker lines, in this simulation. The notochord is represented using elements which produce an axial elongation force, F_{EL} per

element over N_{EL} elements, are separated from each other by distance w and produce a total dimensionless force F_E given by

$$F_E = \frac{N_{EL}\, F_{EL}}{\mu w h \theta}. \quad (6)$$

These elements are shown by the thicker lines just inside the dorsal border of the embryo illustrated in Fig. 3. Again, comparison with biological patterns of deformation make it possible to estimate this force parameter to be approximately F_E=12. The notochord geometry is based on that shown by Youn et al. (1980).

Significant flattening occurs in the dorsal region which overlies the notochord (Fig. 3B). This is not caused by notochord straightening, per se, because the notochord is assumed to have zero bending stiffness in our simulations. The location and degree of the resulting flattening in the virtual embryo is consistent with typical amphibian embryos (Bordzilovskaya et al., 1989). As expected, neither dorsal flattening nor keyhole in-plane shaping occur in simulations where only microfilament forces act.

Transverse aspects of neural tube morphogenesis

To investigate the transverse aspects of neural tube development, we model a narrow transverse strip of the embryo.

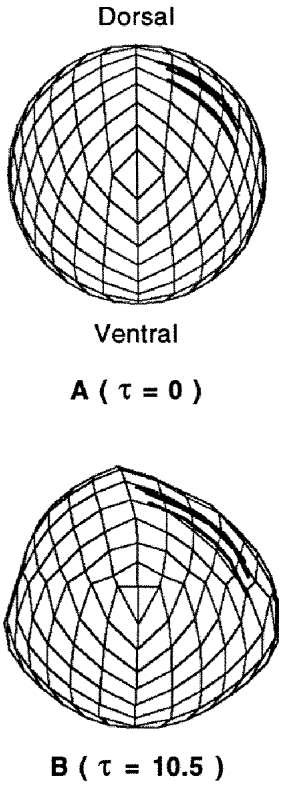

Fig. 3. In the simulation shown here, both notochord and apical forces act on a spherical virtual embryo. The left side of an embryo has been modelled and the cephalic end of the embryo is towards the left in the figure. Finite elements that simulate notochord elongation are shown with heavy lines. The dorsal surface flattens in the region where active notochord elongation occurs.

The use of narrow strips to model transverse shape changes is well established (Odell et al., 1981; Dunnet et al., 1991). We have confirmed the validity of this approach by modelling longer segments of the neural plate. We have also previously shown that the same basic patterns of shape change occur in initially flat (chick) and initially curved (amphibian) virtual neural plates (Clausi, 1991). Here, we use a 'generic' initially flat plate so that no features of the resulting shape changes are attributable to initial curvature effects.

An assemblage of 20 volume finite elements, each 40 μm by 40 μm by 120 μm tall, is used to model a strip from the left half of a neural plate and 20 geometrically identical elements model the attached non-neural ectoderm (Fig. 4). Thicker lines are used to indicate the locations of active CMBs. These forces increase as the microfilament shortens, in accordance with equation (1). Time-lapse images of axolotl neurulation taken in our laboratory and the kinematic maps of Burnside and Jacobson (1968) indicate that the epithelium moves medially. Thus, in the simulation, the left edge of the strip is moved medially at a rate of 56 μm·θ and the strip undergoes uniform axial elongation so that its width doubles by τ=17. This rate of medial motion does not produce compression in the non-neural ectoderm and, therefore, does not drive neural tube closure. All edges of the strip are constrained against rotation.

Fig. 4A shows the starting configuration of the simulation. Fig. 4B,C shows the formation of a distinct neural ridge. As noted by Brodland and Clausi (1993), this is a boundary layer phenomenon. The virtual plate remains largely flat, while it thickens and narrows. This pattern is consistent with a large body of experimental evidence (Burnside and Jacobson, 1968; Burnside, 1973; Brun and Garson, 1983). Fig. 4D-F shows further narrowing and thickening of the plate and the formation of a further 'wedge' or 'hinge' point near the midline (Schoenwolf et al., 1988). One of the important details of this simulation is the occurrence of skewing at the junction between the neural ridges and the rest of the plate (Jacobson et al., 1986; Brodland and Shu, 1992). The neural tube eventually closes (Fig. 4F). When axial elongation occurs, each area of the plate and non-neural ectoderm must thin or narrow so as to maintain constancy of volume (Burnside and Jacobson, 1968), an effect described by Poisson's ratio (Beer and Johnson, 1992). For this reference case, approximately 400 time steps are used.

Are similar patterns of shape change produced by other driving forces? Fig. 5 contains selected, representative time steps from several simulations designed to answer this question. Each simulation is designed to test a particular hypotheses about the forces which drive neurulation, or to determine the sensitivity of the mechanical system to changes in various parameters. The initial geometries and parameters used in these simulations are identical to those used in the reference case except for the alteration of one or two parameters or driving forces as shown in Table 1.

Substantial differences between the simulations are apparent. When no axial elongation occurs (Fig. 5B), both the neuroepithelium and non-neural ectoderm are thicker than in the reference case (Fig. 5A). This, presumably, is

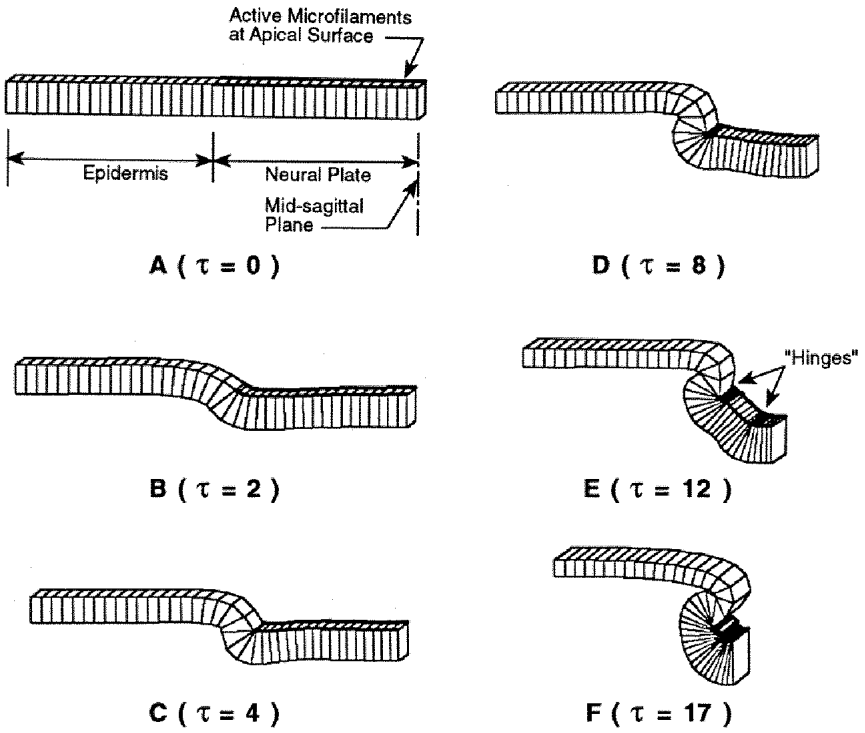

Fig. 4. A reference case simulation of a transverse strip of tissue driven by apical microfilament bundle constriction. The strip is subject to axial elongation and lateral boundary motions as specified in the text. Only the left side of the embryo is shown since the patterns of deformation are symmetric. Three-dimensional views are shown so that the degree of axial elongation is visible.

because Poisson thinning does not occur. If the microfilament force remains constant as described by equation (2) rather than increasing with element shortening, a hinge does not form at the midline and no part of the plate remains flat (Fig. 5C). Even over the extended period of this simulation, a closed neural tube does not form. If the neural plate begins half as thick as in the reference case, a sharper and narrower neural ridge is formed, the midline hinge forms twice as quickly and an additional hinge forms (Fig. 5D). These four simulations suggest that details of the geometry and force generators can significantly affect the shape changes produced.

It is widely held that paraxial microtubules play an important role in neural tube closure (Burnside, 1973; Nardi, 1981; Schoenwolf and Smith, 1990). That paraxial microtubules can influence neural plate thickening and narrowing has been established (Schoenwolf and Powers, 1987). However, their role in neural tube closure has remained unresolved. Another popular and related hypothesis is that adhesion forces drive neurulation (Nardi, 1981). Since the forces produced by paraxial microtubules are mechanically equivalent, both at a cellular and bulk scale, to those produced by intercellular adhesions (Brodland and Clausi, 1993), both hypotheses can be tested using a single simulation. We call these forces transverse forces.

Fig. 5E shows the results of a simulation which is identical to the reference case except that the apical forces are replaced with transverse forces of magnitude F_T=0.04. Other simulations, not included here, show that it is possible for the virtual neural plate to actually thin if the transverse forces are not strong enough to overcome Poisson thinning caused by axial elongation. No tendency towards invagination or rolling is observed. The simulations produce shape changes that resemble those shown in Fig. 6A of Nardi (1981) but not those of his Fig. 6B. We note, however, that if adhesion forces were preferentially directed towards the apical surface, they might cause invaginations. Fig. 5F shows the effect of transverse forces and apical forces acting together. In this case, the virtual neural plate thickens to the point that even when the element apices shrink maximally, they are not sufficiently keystoned to bring about closure.

A related hypothesis, which has been suggested by Nardi (1981) and others, is that transverse forces would cause invaginations to form if an incompressible base is formed by, for example, an extracellular matrix (ECM). We agree that these forces would produce curling in an isolated piece of tissue. However, the simulation shown in Fig. 5G demonstrates that the bending forces that are produced are insufficient to overcome the mediolateral in-plane tension and cause rolling.

Several lines of argument suggest that forces extrinsic to the neural plate might be available to drive neurulation (Schoenwolf and Smith, 1990). The simulation shown in Fig. 5H shows the shape change produced by a medial force of magnitude

$$F_M = \frac{F_{Medial}}{\mu w h \theta} = 0.15, \qquad (7)$$

applied at the lateral edge of the virtual neural plate. We note that the shape produced bears a strong resemblance to the shape that occurs in chick when it is treated with cytochalasin D to disable microfilament action (Schoenwolf and Smith, 1990).

A number of experiments in which neural plate tissue has been implanted into non-neural ectoderm or vice versa have been carried out (Jacobson and Gordon, 1976; Moury and

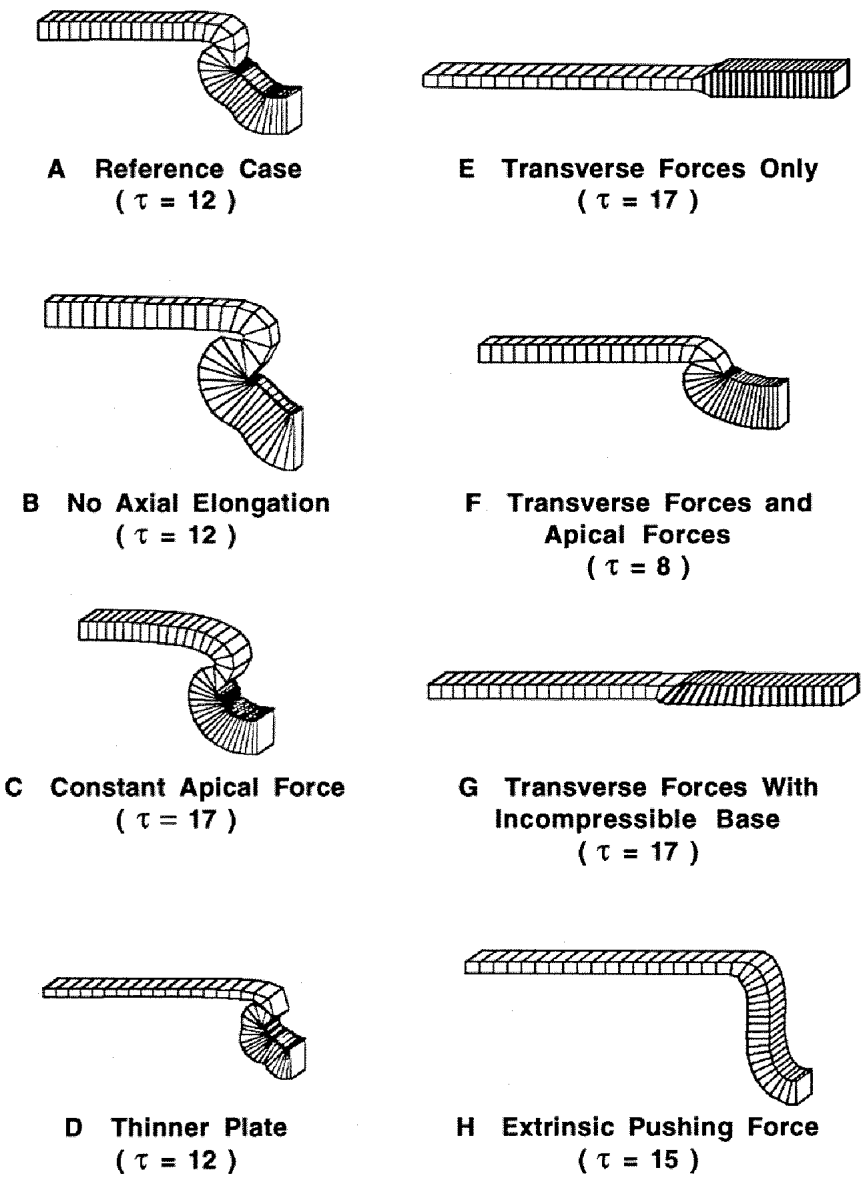

Fig. 5. Representative time steps selected from several families of simulations. Parameter values and other details of the simulations are given in the text and in Table 1. (A) Reference case; (B) no axial elongation; (C) constant apical force; (D) thinner plate; (E) transverse forces only; (F) transverse forces and apical forces; (G) transverse forces with incompressible base; (H) extrinsic pushing force.

Jacobson, 1989). Moury and Jacobson note that 'folds develop at all the new boundaries' and that 'artificially created neural folds always 'roll' over the neural plate.' Fig. 6 shows a simulation in which an 'L'-shaped patch of neural tissue is implanted into non-neural ectoderm cells. The elements shown are 40 μm by 40 μm by 120 μm tall. The neural tissue is different from the non-neural ectoderm only because of its active microfilament forces (F_A=0.10), shown with thicker lines. The simulation shows that the rolling follows the newly formed boundary closely. Other details of the shape change are apparent in cross-sectional views of invagination driven by similar forces and shown in Brodland

Table 1. Parameters used in transverse section simulations

Simulation name	Initial thickness (μm)	Axial elongation	Apical force F_A	Transverse force, F_T	Other properties
Reference case	120	Yes	0.10 (Eqn 1)	0	–
No axial elongation	120	No	0.10 (Eqn 1)	0	–
Constant apical force	120	Yes	0.10 (Eqn 2)	0	–
Thinner plate	60	Yes	0.10 (Eqn 1)	0	–
Transverse forces	120	Yes	0	0.04	–
Transverse forces andapical forces	120	Yes	0.10 (Eqn 1)	0.04	–
Transverse forces with incompressible base	120	Yes	0	0.04	Incompressible base
Extrinsic pushing forces	120	Yes	0	0	Extrinsicforces

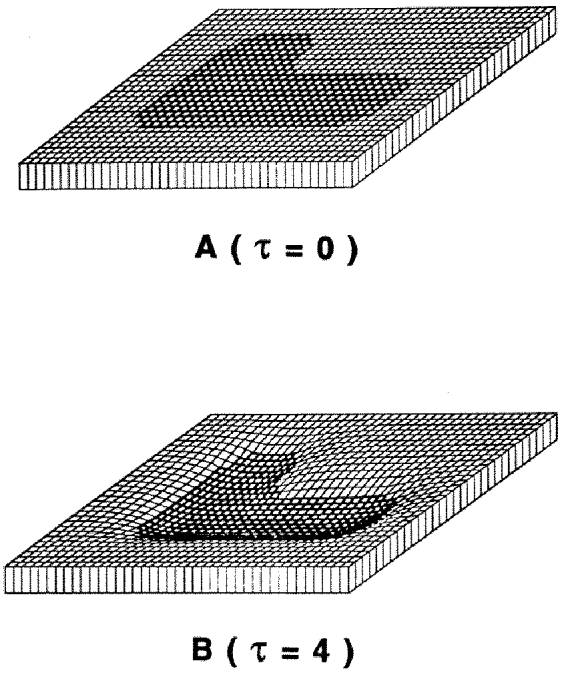

Fig. 6. This simulation shows an 'L'-shaped piece of neural tissue (tissue in which CMBs are assumed to be active) implanted into non-neural ectoderm. Note how rolling of the non-neural ectoderm onto the implanted neural tissue occurs along the boundary between the two tissue types.

and Clausi (1993). Thickening of the neural tissue, edge rolling and the occurrence of a somewhat flattened bottom are evident.

DISCUSSION

Simulations of the type presented here can have two interpretations. They can be used to test hypotheses about the forces that drive neurulation. They can also predict how perturbations to driving forces would affect the patterns shape changes produced. The simulations show that the kinds of shape change produced in a virtual neural plate are highly sensitive to the *sources* of the driving forces (Fig. 5A,E,H) and to their details (Fig. 5C,F) making analyses based on either interpretation meaningful. In contrast, when only the ratio of driving force to element viscosity is increased, accelerated sequences of otherwise identical shape change are produced (Brodland and Clausi, 1993).

To compare models that differ in geometry, however, is less straightforward (Brodland, 1988). Nonetheless, it can be concluded from the numerous simulations that we have done, some of which are shown herein, that CMB constriction acting alone or in concert with other force generators has a strong tendency to produce the characteristic features of neural tube closure in virtual embryos of various geometries (Fig. 5A-D,F). Thus, the simulations suggest that, even in species that have substantially different neural plate geometries, CMB constriction is likely the principal driving force.

The reference case simulation demonstrates that isotropic apical constrictions, which increase with shortening microfilament length in accordance with equation 1, can, by themselves, produce the cardinal transverse features of neurulation in a virtual neural plate. These include the successive formation of distinct neural ridges, thickening and narrowing of the neural plate, skewing of cells at the medial edge of the neural ridges, formation of distinct hinge points, and rolling and closure of the neural tube. Here, no use is made of cell 'programs,' cortical tractoring (Jacobson et al., 1986), or biochemical controls or signals.

The mechanical basis of this sequence of shape changes can be explained in detail. Initially, the apical forces in the neural plate are balanced from element to neighbouring element (or cell to neighbouring cell) everywhere except at the junction of the neural plate and the non-neural ectoderm (Fig. 4A). This allows the cells at the lateral edge of the neural plate to constrict apically, become keystone-shaped and form a distinct boundary layer, which we recognize as the neural ridge (Brodland and Clausi, 1993). Neighbouring non-neural ectoderm cells are, in response, drawn over the edge of the neural plate (Fig. 4B,C). Tension in the ectodermal sheet regulates the degree of rolling at the boundary layer and causes the rest of the ectoderm to remain flat. That this is indeed a boundary layer phenomenon is supported by the simulation shown in Fig. 6.

As the apices of the neural plate cells continue to constrict, the neural plate narrows and thickens, and the microfilament force acts even further from the current middle surface (Flugge, 1973) of the sheet (Fig. 4D). As the microfilaments constrict, the microfilament force also increases in accordance with equation (1). As a result of these two factors, a substantially increased bending moment is produced leading to neural tube closure (Fig. 4F). That closure is substantially delayed or possibly prevented when the microfilament force does not increase (Fig. 5C) and that closure of a thicker plate, which has the same total volume, is accelerated (Fig. 5B), support this interpretation. The thinner plate (Fig. 5D) closes more quickly because the ratio of forces acting to the amount of cellular material that must be deformed is substantially higher and thus does not contradict this conclusion.

The data of Burnside and Jacobson (1968) show that the cephalic end of the future spinal region undergoes less axial elongation and is thicker than the balance of the future spinal region of the plate. The simulations suggest that this short section of the tube closes first because of its greater thickness. The cephalic parts of the plate do not close as quickly even though they are thicker because they do not benefit from Poisson narrowing caused by axial elongation.

The degree of curvature produced is not uniform from point to point across the width of the plate. Schoenwolf et al. (1988) refer to the regions where concentrated bending occurs as hinge points. That these hinge points are indeed caused by the same kind of mechanical instability as that discussed by Brodland and Clausi (1993) is strongly indicated by the constant force (Fig. 5C) and thinner plate (Fig. 5D) simulations. In the thinner virtual plate, hinge spacing is sufficiently reduced that an additional hinge is produced. Also, consistent with the predictions of Brodland and Clausi, when a constant force (equation (2)) is used, no hinges form.

The simulations show that transverse forces alone will not drive neural ridge formation or produce tube closure in virtual embryos (Fig. 5E,G). They do, however, cause plate thickening and narrowing. This is consistent with experiments in which microtubule inhibitors are applied and normal plate thickening and narrowing does not occur (Schoenwolf and Powers, 1987). Whether microtubules provide an active driving force or whether they act to stabilize shape changes driven by other mechanisms (Gordon and Brodland, 1987) is unknown. If the transverse force were increased, an identical sequence of shape changes would be produced, but at a faster rate.

The extrinsic pushing force simulation (Fig. 5H) demonstrates that neurulation-like motions that match those reported by Schoenwolf and Smith (1990) would occur if lateral pushing forces act at the edge of the neural plate. Schoenwolf et al. (1988) report that neurulation-like motions can occur in the absence of apical microfilaments. Lateral forces, generally similar to those used in this simulation, might be produced by other means. For example, when the neural plate is removed, medial motions can still occur, but these motions are somewhat retarded (Jacobson, 1962; Jacobson and Jacobson, 1973). That the archenteron roof has the ability to drive morphogenetic motions is clear from Fig. 5 of Jacobson and Löfberg (1969) where, in the caudal region, the mesoderm motions occur at a faster rate than those of the immediately overlying neural plate. The medial motions of the ectoderm are apparently driven by medial motions of the mesoderm and endoderm, for in the absence of these tissues ‘neurulation movements were inhibited entirely’ (Jacobson, 1962).

Experiments in which slits are made in the neural plate or adjoining non-neural ectoderm (Lewis, 1947; Jacobson, 1962; Karfunkel, 1974; Jacobson and Gordon, 1976) have led to the conclusion that the ectoderm is under considerable tension. Closure and healing of the slits, a process that takes of the order of one hour, is apparently a wound healing reaction. Schoenwolf and Smith (1990) argue that such gaping is due to extrusion of deep cells and that slit closing is the result of compressive extrinsic forces in the epithelium. This, however, is not consistent with Jacobson (1962), who reported that when a long incision is made through both the neural plate and the archenteron roof, the separated portions of the neural plate narrow and the gap continues to widen. Apparently, wound healing mechanisms are insufficient to close a long gap. If the non-neural ectoderm acted to push the neural folds together, as argued by Schoenwolf and Smith, a long gap should still close. Schoenwolf et al. (1988) suggest that expansion of the surface ectoderm may provide the driving force. The simulation represented in Fig. 5H suggests that such forces, by themselves, would not produce normal patterns of neural tube formation.

The ability of the notochord to cause axial elongation of explanted neural plates is well established (Jacobson and Gordon, 1976; Jacobson, 1984; Adams et al., 1990) and has led to the notion that it generates axial elongation forces in amphibian embryos. Youn and Malacinski (1981), however, report that apparently normal keyhole shape formation and tube closure are possible in notochordless embryos. Since invagination of epithelial tissue through the blastopore continues during the early stages of neurulation, this might drive the axial elongation. Indeed, the axial force that would be produced by invagination of dorsal epithelium would be almost mechanically equivalent to that produced by notochord elongation. The elongation that acts in the simulation shown in Fig. 3 is consistent with either notochord elongation or epithelial invagination through the blastopore. That notochordless explants do not elongate (Jacobson and Gordon, 1976) suggests that differential adhesions between laterally adjacent neural plate cells do not act. If they did, they would produce convergent extension and thus narrow and elongate the excised plate.

In the presented simulations, consistent with the current literature, all neural plate cells are assumed to be initially identical. The gross shape changes and local element-element (cell-cell) differences that develop during the course of the simulations result entirely from mechanical interactions between the elements and not from manual pre-programming (Jacobson and Gordon, 1976) or triggering (Odell et al. 1981). Thus, for example, in a simulation of a notochordless embryo, the substantially different pattern of virtual neural plate thickness changes is determined entirely by mechanical interactions (Figs 2, 5B). In contrast, Jacobson and Gordon use the same pre-programmed height changes for simulations with and without a notochord. Because our simulations treat as unknowns a greater number of relevant primary quantities, such as in-plane displacements and sheet thickness, the likelihood that erroneous driving forces would produce proper shape changes is also reduced.

Inasmuch as the mechanical development that occurs at one instant is dependent on the previous mechanical history of the embryo, a mechanical basis for an epigenetic landscape exists. Critical biochemical consequences may also follow from the mechanical changes (Ben Ze’ev, 1985) and, in turn, may directly affect the characteristics of the epigenetic landscape. Because embryonic cells are in mechanical contact with each other, they can be considered to be sending mechanical signals to each other through force interactions. It is through these ‘signals’ that a mechanical system might contribute to an increase in embryo complexity.

Brodland and Clausi (1993) have demonstrated that apical contraction forces can produce a significant variety of behaviours in cell sheets and masses of cells including invagination, wave propagation and pattern formation. This suggests that a uniformity of causes might exist between these various phenomena. Thus gastrulation, neural tube rolling, wave propagation, optic cup formation and somite formation (Stern and Goodwin, 1977; Jacobson, 1978) might be caused by related mechanisms.

The traditional viewpoint is that neural plate closure is driven by the CMB constriction, paraxial microtubule elongation and notochord-driven axial elongation. Our simulations of transverse sections suggest that CMB constriction and axial elongation are the principal driving forces. Paraxial microtubule elongation, in contrast, can slow or even prevent neural tube closure of virtual embryos. CMB constriction and axial elongation acting together can also produce dorsal surface flattening in amphibians and in-plane shape changes that match closely corresponding time-lapse

sequences. They also produce numerous salient transverse features of normal neurulation.

The possibility that there may be cooperation of forces (Schoenwolf and Smith, 1990; Brun and Garson, 1983), and significant interspecies differences in the forces that act, is also supported by our simulations. The experimental evidence and simulations also suggest that there is redundancy in this mechanical system. Thus, should the primary system not exert sufficient force or cause shape changes to occur at some minimal rate, the action of a secondary system becomes evident. Redundancy is an important feature of complex man-made systems and provides for them the robustness that many natural systems seem to enjoy.

With regard to the role of specific subcellular components in neurulation, we suggest that microfilaments play a primary role in driving the shape changes. Microtubules may, however, act to provide intracellular transport and to stabilize the cells mechanically. They might also mechanically constrain and thus regulate, microfilament-driven motions (Gordon and Brodland, 1987). Intermediate filaments apparently give cell cytoplasm a high effective viscosity and provide lateral support to microtubules (Brodland and Gordon, 1990). We recognize that a host of molecular mechanisms are involved in these mechanical processes. Biochemical and electrical signals within the plate and from tissues adjacent to the neural plate may also be important to certain stages of plate or tube development. This notwithstanding, it is evident that the ultimate processes that bring about neural plate shaping and neural tube closure are mechanical.

We consider the simulations presented here an important step towards a more quantitative understanding of development like that called for by Koehl (1990). Another important step would be the cataloguing of detailed, species-specific mechanical properties on which to base simulations. If the shape changes produced in a particular mechanical simulation do not match experimental results, this would indicate that additional factors are acting. These might include other mechanical factors, biochemical signals, cell programs, or other factors that ultimately have mechanical consequences. Indeed, a next step might be to identify detailed differences between species-specific simulations and corresponding experimental results, and to use these to identify where other factors that have direct mechanical consequences must be at work.

This research was funded a Natural Sciences and Engineering Research Council of Canada (NSERC) research grant to G. W. B. and an NSERC Postgraduate Scholarship to D. A. C. Animals for this study were obtained from the Axolotl Colony of Dr J. B. Armstrong, University of Ottawa.

REFERENCES

Abel, J. F., Kawai, T. and Shen, S-F (eds.) (1981). *Interdisciplinary Finite Element Analysis*. New York: Cornell University.

Adams, D. S., Keller, R. and Koehl, M. A. R. (1990). The mechanics of notochord elongation, straightening and stiffening in the embryo of *Xenopuslaevis*. *Development* **110**, 115-130.

Ben-Ze'ev, A. (1985). Cell-cell interaction and cell configuration-related control of cytokeratins and vimentin expression in epithelial cells and in fibroblasts. *Ann. N.Y. Acad. Sci.* **455**, 597-613.

Beer, F. P. and Johnston, E. R. (1992). *Mechanics of Materials*, 2nd ed. New York: McGraw-Hill Inc.

Bordzilovskaya, N. P., Dettlaff, T. A., Duhon, S. T. and Malacinski, G. M. (1989). Developmental-Stage Series of Axolotl Embryos. In *Developmental Biology of the Axolotl* (ed. J. Armstrong and G. Malacinski). New York: Oxford University Press.

Brodland, G. W. (1988). Highly non-linear deformation of uniformly-loaded circular plates. *Int. J. Solids. Structures* **24**, 351-362.

Brodland, G. W. (1993). Finite element methods for developmental biology. *The Cytoskeleton in Development Biology*. *International Review of Cytology*, Academic Press. In press.

Brodland, G. W. and Clausi, D. A. (1993). Embryonic cell sheet morphogenesis modelled by FEM(In Preparation).

Brodland, G. W. and Gordon, R. (1990). Intermediate filaments may prevent buckling of compressively loaded microtubules. *J. Biomech Eng.* **112**, 319-321.

Brodland, G. W. and Shu, D-W. (1992). Are intercellular membrane forces important to amphibian neurulation? In *Dynamical Phenomena at Interfaces, Surfaces and Membranes* (ed. G. Forgacs and D. Beysens). New York: Nova Science Publishers.

Brun, R. B. and Garson, J. A. (1983). Neurulation in the Mexican salamander (*Ambystoma mexicanum*): a drug study and cell shape analysis of the epidermis and the neural plate. *J. Embryol. Exp. Morph.* **74**, 275-295.

Brun, R. B. and Garson, J. A. (1984). Notochord formation in the Mexican salamander (*Ambystoma mexicanum*) is different from notochord formation in *Xenopus laevis*. *J. Exp. Zool.* **229**, 235-240.

Burnside, B. (1971). Microtubules and microfilaments in newt neurulation. *Dev. Biol.* **26**, 416-441.

Burnside, B. (1973). Microtubules and microfilaments in amphibian neurulation. *Am. Zool.* **13**, 989-1006.

Burnside, M. B. and Jacobson, A. G. (1968). Analysis of morphogenetic movements in the neural plate of the newt Taricha torosa. *Dev. Biol.* **18**, 537-552.

Burt, A. (1943). Neurulation in mechanically and chemically inhibited Amblystoma. *Biol. Bull.Mar. Biol. Lab., Woods Hole* **85**, p. 108.

Campbell, L. R., Dayton, D. H. and Sohal, G. S. (1986). Neural tube defects: a review of human and animal studies on the etiology of neural tube defects. *Teratology* **34**, 171-187.

Cheng, L. Y. (1987a). Deformation analyses in cell and developmental biology. Part I - Formal methodology. *J. Biomech. Eng.* **109**, 10-17.

Cheng, L. Y. (1987b). Deformation analyses in cell and developmental biology. Part II - Mechanical experiments on cells. *J. Biomech. Eng.* **109**, 18-24.

Clausi, D. A. (1991). *Finite Element Simulations of Early Embryonic Development.* M.A.Sc. Thesis, University of Waterloo.

Copp, A. J., Brook, F. A., Estibeiro, P., Shum, A. S. W. and Cockroft, D. L. (1990). The embryonic development of mammalian neural tube defects. *Progress in Neurobiology* **35**, 363-403.

Dunnett, D., Goodbody, A. and Stanisstreet, M. (1991). Computer modelling of neural tube defects. *Acta Biotheoretica* **39**, 63-79.

Flugge, W. (1973). *Stresses in Shells*, 2nd ed. Berlin: Springer-Verlag.

Gordon, R. (1985). A review of the theories of vertebrate neurulation and their relationship to the mechanics of neural tube birth defects. *J. Embryol. Exp. Morph.* **89 Supplement**, 229-255.

Gordon, R. and Brodland, G. W. (1987). The cytoskeletal mechanics of brain morphogenesis: cell state splitters and primary neural induction. *Cell Biophys.* **11**, 177-237.

Gordon, S. R. and Essner, E. (1987). Investigation on circumferential microfilament bundles in rat retinal pigment epithelium. *European J. Cell Biol.* **44**, 97-104.

Hilfer, S. R. and Hilfer, E. S. (1983). Computer simulation of organogenesis: An approach to the analysis of shape changes in epithelial organs. *Dev. Biol.* **97**, 444-453.

Hiramoto, Y. (1969). Mechanical properties of the protoplasm of the sea urchin egg. - I. Unfertilized Egg. *Exp. Cell Res.* **56**, 201-208.

His, W. (1874). *Unsere Körperform und das physiologische problem ihrer enstehung, briefe an einen befreundeten naturforscher*. Leipzig: F.C.W. Vogel.

Jacobson, A. G. (1978). Some forces that shape the nervous system. *Zoon* **6**, 13-21.

Jacobson, A. G. (1980). Computer modelling of morphogenesis. *Am. Zool.* **20**, 669-677.

Jacobson, A. G. (1984). Further evidence that formation of the neural tube requires elongation of the nervous system. *J. Exp. Zool.* **230**, 23-28.
Jacobson, A. G. and Gordon, R. (1976). Changes in the shape of the developing vertebrate nervous system analyzed experimentally, mathematically and by computer simulation. *J. Exp. Zool.* **197**, 191-246.
Jacobson, A. G., Oster, G., Odell, G. M. and Cheng, L. Y. (1986). Neurulation and the cortical tractoring model for epithelial folding. *J. Embryol. Exp. Morph.* **96**, 19-49.
Jacobson, C. O. (1962). Cell migration in the neural plate and the process of neurulation in the axolotl larva. *Zool. Bidrag, Uppsala* **30**, 433-449.
Jacobson, C. O. and Jacobson, A. (1973). Studies on morphogenic movements during neural tube closure in amphibia. *Zoon* **1**, 17-21.
Jacobson, C. O. and Löfberg, J. (1969). Mesoderm movements in the amphibian neurula. *Zool. Bidrag, Uppsala* **38**, 233-239.
Karfunkel, P. (1974). The mechanisms of neural tube formation. *Int. Rev. Cytol.* **38**, 245-271.
Keeton, W. T. and Gould, J. L. (1986). *Biological Science*, 4th ed. New York: W.W. Norton and Company.
Koehl, M. A. R. (1990). Biomechanical approaches to morphogenesis. *Seminars in Developmental Biology*, Vol. **1**, 367-378.
Lee, H. and Nagele, R. G. (1988). Intrinsic forces alone are sufficient to cause closure of the neural tube in the chick. *Experientia* **44**, 60-61.
Lewis, W. H. (1947). Mechanics of invagination. *Anat. Rec.* **97**, 139-156.
Moury, J. D. and Jacobson, A. G. (1989). Neural fold formation at newly created boundries between neural plate and epidermis in the axolotl. *Dev. Biol*. **133**, 44-57.
Nagele, R. G. and Lee, H. (1980). Studies on the mechanism of neurulation in the chick microfilament-mediated changes in cell shape during uplifting of neural folds. *J. Exp. Zool.* **213**, 391-398.
Nardi, J. B. (1981). Epithelial invagination: Adhesive properties of cells can govern position and directionality of epithelial folding. *Differentiation* **20**, 97-103.
Odell, G. M., Oster, G., Alberch, P. and Burnside, B. (1981). The mechanical basis of morphogenesis, I. Epithelial folding and invagination. *Dev. Biol.* **85**, 446-62.
Phillips, H. M. and Steinberg, M. S. (1978). Embryonic tissues as elastoviscous liquids, I. Rapid and slow shape changes in centrifuged cell aggregates. *J. Cell Sci.* **30**, 1-20.
Rappaport, R. (1977). Tensiometric studies of cytokinesis in cleaving sand dollar eggs. *J. Exp. Zool.* **201**, 375-378.
Roux, W. (1888). Beiträge zur entwickelungsmechanik des embryo. Über die künstliche hervorbringung halber embryonen durch zerstörung einer der beiden ersten furchungskugeln, sowie über die nachentwickelung (postgeneration) der fehlenden körperhälfte. *Virchows Arch. path Anat. u. Physiol. u. kl. Med.* **114**, 113-153, 289-291.
Schoenwolf, G. C., Folsom, D. and Moe, A. (1988). A reexamination of the role of microfilaments in neurulation in the chick embryo. *Anat. Rec.* **220**, 87-102.
Schoenwolf, G. C. and Powers, M. L. (1987). Shaping of the chick epithelium during primary and secondary neurulation: Role of cell elongation. *Anat. Rec.* **218**, 182-195.
Schoenwolf, G. C. and Smith, J. L. (1990). Mechanisms of neurulation: traditional viewpoint and recent advances. *Development* **109**, 243-270.
Smith, J. L. and Schoenwolf, G. C. (1991). Further evidence of extrinsic forces in bending of the neural plate. *J. Comp. Neurol.* **307**, 225-236.
Stern, C. D. and Goodwin, B. C. (1977). Waves and periodic events during primitive streak formation in the chick. *J. Embryol. Exp. Morph.* **41**, 15-22.
Trinkaus, J. P. (1984). *Cells into Organs, the Forces that Shape the Embryo*. 2nd ed. Englewood Cliffs, NJ: Prentice-Hall.
Weliky, M. and Oster, G. (1990). The mechanical basis of cell rearrangement I. Epithelial morphogenesis during Fundulus epiboly. *Development* **109**, 373-386.
Youn, B. W. and Malacinski, G. M. (1981). Axial structure development in ultraviolet-irradiated (notochord-defective) amphibian embryos. *Dev. Biol.* **83**, 339-352.
Youn, B. W., Keller, R. E. and Malacinski, G. M. (1980). An atlas of notochord and somite morphogenesis in several anuran and urodelean amphibians. *J. Embryol. Exp. Morph.* **59**, 223-247.
Zienkiewicz, O. C. and Taylor, R. L. (1989). *The Finite Element Method, Basic Formulation and Linear Problems.* Fourth Edition, Vol. 1, McGraw-Hill, London.
Zienkiewicz, O. C. and Taylor, R. L. (1991). *The Finite Element Method, Solid and Fluid Mechanics Dynamics and Non-Linearity.* Fourth Edition, Vol. 2, McGraw-Hill, London.

(Accepted 15 March 1993)